3D Graphene Nanocomposite by Electrospinning for Supercapacitor

Saptarshi Dhibar and Sudip Malik

Abstract In the present scenario, development of green and sustainable energy sources becomes an enormous challenge due to the rising environmental problems and diminution of natural energy sources like gas, coal and oil. To fulfill the requirement researchers from all over the world have typically focused on the development of various energy storage devices like accumulators, capacitors, batteries as well as supercapacitors utilizing different functional materials. Graphene, a novel type nano-sized carbon, has drawn significant research interest as an electrode material for supercapacitor due to its superior properties like high mechanical strength, better electrical conductivity, good chemical stability, excellent flexibility, as well as board electrochemical windows. For the fabrication of nanofiber, electrospinning technique has been known as the main adaptable as well as versatile technique. To enhance high energy storage capacity along with the environment impact of electrospun supercapacitors, researchers have widely established original resolution for storing and harvesting energy from nanofiber. The present chapter presents a clear overview of the electrospinning processes, the basic concept of the supercapacitor electrode materials and 3D graphene-based nanocomposites via electrospinning techniques for the electrode materials for supercapacitor.

Keywords Electrospinning · Supercapacitors · 3D graphene architectures · 3D graphene-based electrode materials

1 Introduction

The electrochemical energy storage techniques including batteries, electrochemical capacitors as well as fuel cells are opening a new impact in our lives, as nearly all the

S. Dhibar (✉) · S. Malik
School of Applied and Interdisciplinary Sciences, Indian Association for the Cultivation of Science, 2A & 2B Raja S. C. Mullick Road, Jadavpur, Kolkata 700032, India
e-mail: saptaaus2007@gmail.com

S. Malik
e-mail: psusm2@iacs.res.in

S. K. Tiwari et al. (eds.), *Electrospinning of Graphene*, Carbon Nanostructures,
https://doi.org/10.1007/978-3-030-75456-3_4

past sources of energies (like, wind power, hydropower, solar energy, bio-energy etc.) are intermitted in nature [1, 2]. Generally, the electrochemical capacitors also known as ultracapacitor or supercapacitors are the energy storage devices that can storage as well as release the electrical energy through very fast charge/discharge rates. These are also having higher power densities, lower maintenance cost, excellent cyclic life span and safe operation [3–6]. Due to these excellent properties, supercapacitors are potentially useful in various fields like in portable electronics, in vehicles, in memory backup systems as well as in different electronics industries.

Based on the charge storage mechanism, supercapacitor has been divided into two categories, pseudocapacitors as well as electrochemical double layer capacitors (EDLC). The pseudocapacitors materials can store the charge via reversible redox reactions taken place in between electrolytes in addition to electrode materials, involving oxidation–reduction and electrosorption reaction procedures. It is well known fact that more charge can be stored in pseudocapacitor materials as compared to EDLC materials because the electrochemical techniques can arise not only on the surface of the electrode materials but also in the bulk of the electrode materials. On the other hand, the EDLC materials can store the electric charges on the electrode surface along with the opposite charged ions on the electrolyte side via reversible ion adsorption/desorption technique. The EDLC materials exhibit exclusive power performance along with enormously long cycle lifetime because the electrostatic charge storage technique not only promises quick energy uptake and delivery, but also prevents the swelling of electrode materials. Carbonaceous materials are mostly utilized for the promising candidates for the EDLC materials due to their higher surface area, good electrochemical stability in solutions, superior conductivity etc. [7].

Nanofibers are fabricated by different synthetis techniques, such as by template synthesis of nano-structured polymers, self-assemble, phase separation as well as by electrospinning techniques [8, 9]. Out of which, more adaptable and unique methods for the fabrication of the nano and macro fibers are via electrospinning techniques that has become a universal technique in the area of nanotechnology [10, 11]. Most of the one-dimensional (1D) nanofibers with repeated tenability can be developed with the help of these electrospinning techniques. Compared to economical mechanical spinning technique for producing the microfibers, electrospinning technique largely makes use of the electrostatic repulsion among surface charges to diminish the diameter of a viscoelastic jet or a glassy filament. On the other hand, the electrospinning technique is comparatively easier as well as non-expensive which has the most significant advantages for the production of huge number of various kinds of nanofiber by this technique. In addition to this, other benefits of this technique are that it has the capability to control the diameters of the fiber, high aspect ratio, high surface-to-volume ratio in addition to pore size as non-woven fabrics. Due to these significant properties, the nanofibers fabricated by electrospinning technique have shown enormous potential in the field of electrode materials for supercapacitors. Many researches have already been performed on the fabrication of nanofiber, nanotubes, hierarchical nanomaterials along with coaxial nanocables that have used the electrode materials for the supercapacitors [12–15]. It has also noticed that day by day the number of publications has been rising on the field of nanomaterials prepared by electrospinning

techniques for the supercapacitor electrode materials. This chapter is proposed the present research activities in the field of 3D graphene-based nanomaterials fabricated by the help of electrospinning techniques for the electrode materials for supercapacitor. The basic concept of supercapacitors and their classifications, fundamental of electrospinning including electrospinning process, and the nanocomposites produced via electrospinning process has elaborately discussed.

2 Supercapacitor

Supercapacitors also known as ultracapacitor or double-layer capacitor are mainly the electronic devices that have been utilized to store enormously huge amount of electrical charge in the electrical double layer formed at the interface of electrode materials and electrolytic solutions [2]. Their stored energy is typically 10 to 100 times more energy per unit volume or mass as compared to electrolytic capacitors. Due to its simpler and fast charging as well as faster delivery of charge, it has been preferred to batteries. The capacitance reached by utilizing the help of this technology can be as high as 12,000 F. The self-capacitance of the whole planet Earth is barely about 710 μF, that values is 15 million times less than as compared to the capacitance of a supercapacitor. Supercapacitors are generally polar devices, like electrolytic capacitors they have to be linked to the circuit. The charge discharge times for supercapacitors are equivalent to ordinary capacitors. Due to their comparatively low internal resistance, it is feasible to reach high charge discharge current. In case of battery, to reach fully charge state it takes several hours whereas in case of supercapacitors to reach the charge state it takes less than a few minutes. The specific power of supercapacitors is relatively high as compared to the batteries. It is observed that the specific powers of Li-ion batteries are in between 1 and 3 kW/kg and the supercapacitors have a specific power of roughly ~10 kW/kg. This high specific power helps supercapacitors in some of the important applications where quick busts of energy are required in a short period of time. Supercapacitors have excellent life cycles, generally millions of times of charge and discharge cycles. On the other hand, battery has the maximum life cycles of 500 or more than that.

As like electrolytic capacitors, the supercapacitor has been constructed and it contains two foil electrodes, a separator along with an electrolyte. Generally, the separator is placed in between the two electrodes to make sandwiched structure and finally rolls as rectangular or cylindrical in shape. The electrodes and the electrolytes which have been used for the fabrication of supercapacitors are completely dissimilar from those which have been utilized in normal electrolytic capacitors. A schematic representation of a supercapacitor has been illustrated in Fig. 1a. It stores the electrical energy inside the electrical double layer close to the surface having high surface area materials inside an electrode. At the time of charging of the supercapacitors, the anions as well as the cations are moved towards the electrode surface on the suitable surface of the cell. Differing surface charges on the electrodes equilibrium

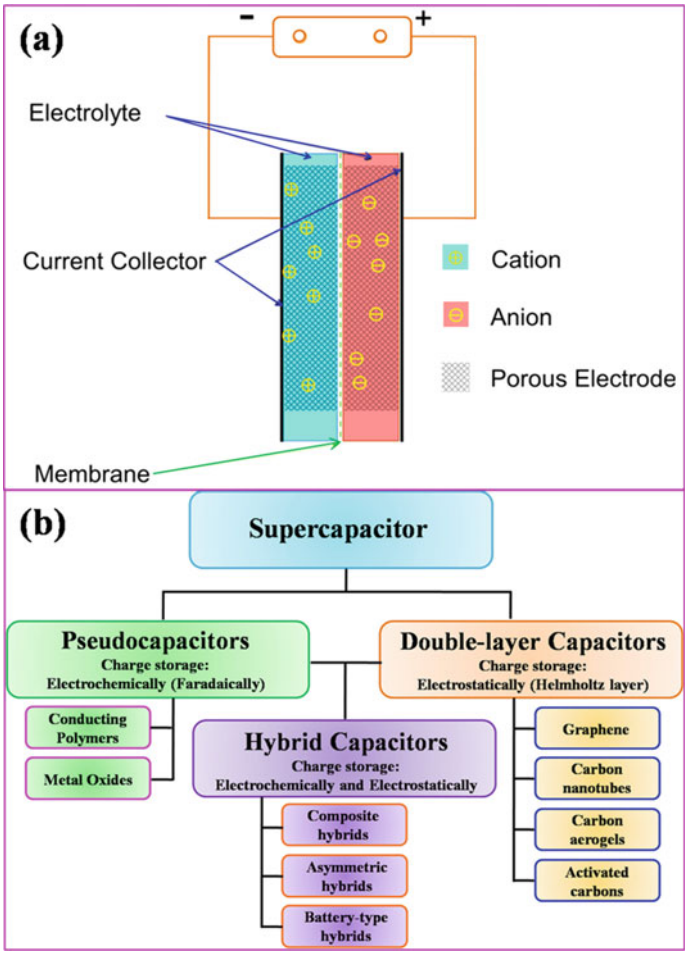

Fig. 1 **a** Schematic representation of a supercapacitor, **b** classification of supercapacitor. Reproduced from Ref. [16]

the electric field produced through the concentrated ions close to the surface, developing a potential difference among the two electrodes. At the time of discharging, the potential difference slowly reduces when ions move away from the surfaces of the electrode, and ultimately, the last result is a neutral electrolyte having least concentration gradient from the cathode and anode [16]. Concentrations of ions in the electrolyte as well as the complete active surface area inside the electrodes are the two important factors that determine the entire charge capacity along with the energy density.

Supercapacitor has numerous advantages such as, due to its low resistance it can deliver high power and allow high load current. The charging mechanism of a supercapacitor is very simple and fast and also is not cause to undergo overcharging.

As compared to batteries, a supercapacitor has marvellous low and high temperature charge along with discharge performance. Supercapacitor has also low impedance value and is extremely reliable. Apart from these good advantages, it has some disadvantages also, such as, high fabrication cost, high self-discharge, low specific energy, along with linear discharge voltage. Supercapacitors have been classified into three categories, such as pseudocapacitors, electrochemical double layer capacitors (EDLC), and hybrid capacitors. The classifications of the supercapacitors have been summarized in Fig. 1b.

2.1 Pseudocapacitors

The pseudocapacitors can store electrical energy faradaically through electron charge transfer between electrodes as well as electrolytes. This is achieved by oxidation–reduction reactions (redox reactions), electrosorption, along with intercalation processes, known as pseudocapacitance. The electrons which are engaged in the faradaic processes are transported to or from valance electron states of the redox electrode reagent. They go into the negative electrode and flow via the external circuit to the positive electrode in which a second double layer with an equivalent number of anions has produced. The electrons which arrive at the positive electrode are not moved to the anions forming the double layer, rather they can stay in the strongly ionized as well as 'electron hungry' transition metal ions of the electrode's surface.

The capability of electrodes to achieve pseudocapacitance effects by redox reactions, intercalation or electrosorption powerfully rely upon the chemical affinity of the electrode materials to the ions absorbed on the surface of the electrode along with the dimension and structure of the pores of the electrodes. Materials undergoing such redox behavior include: (i) conducting polymers, such as polyaniline, polypyrrole, polythiophene etc., (ii) transition metal oxides, like MnO_2, RuO_2, IrO_2, Co_3O_4 etc. (iii) transition metal sulfide, as well as (iv) mixed transition metal oxide and sulfides [17–26]. It is also reported that the RuO_2 is one of the most efficient electrode materials for pseudocapacitor because of its superior conductivity as well as distinct multiple reversible redox states available inside a potential window of 1.2 V. Pseudocapacitor mainly shows three types of faradaic processes such as reversible electrochemical doping-dedoping in conducting polymer based electrode, redox reactions of transition metals oxides, as well as reversible absorption (such as, adsorption of hydrogen on the surface of gold or platinum). It has also been studied that the faradaic electrochemical techniques not only enlarge the working voltages but also enhance the specific capacitance of the supercapacitors. Pseudocapacitor exhibits better specific capacitance values as well as energy density as compared to EDLC because the electrochemical processes take place both on the surface as well as in the bulk close to the surface of the solid electrode. It is also reported that the capacitance of the pseudocapacitor can be 10–100 times higher than that of electrostatic capacitance of an EDLC. Though, it suffers from comparatively lower power density compared

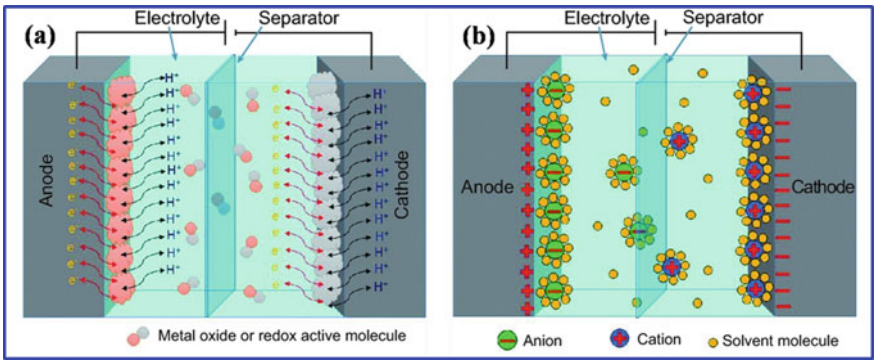

Fig. 2 Schematic representation of **a** a pseudocapacitor and **b** an electrochemical double layer capacitor. Reproduced from Ref. [27]

to EDLC as faradaic processes are generally slower than nonfaradaic processes. Further, as redox reactions take place at the electrode, a pseudocapacitor frequently lacks stability at the time of cycling. Therefore, the cyclic stability of a pseudocapacitor is less as compared to EDLC. A schematic representation of a pseudocapacitor is represented in Fig. 2a.

2.2 Electrochemical Double Layer Capacitor (EDLC)

In an electrostatic or EDLC, the capacitance of the electrode/interface is connected to an electrode-potential-dependent accumulation of charge at the interface. The mechanism of surface electrode charge generation comprises ion adsorption along with surface dissociation from both the crystal lattice defect as well as electrolytes [3]. These processes function exclusively on the electrostatic accretion of surface charge. The EDLC comes from electrode materials particles, for example at the interface among the carbon particles as well as the electrolyte, in which an excess or a shortage of electric charge is built up on the surface of the electrode, and electrolyte ions with counterbalancing charge are accumulated on the electrolyte side in order to meet the electro-neutrality. At the time of charging, the electrons are moved from the negative electrode to the positive electrode via an external load. Inside the electrolyte, anions are migrated towards the positive electrode whereas the cations are migrated towards the negative electrode. At the time of discharging, opposite processes happen. In this category of supercapacitors, there is no charge transfer in between the electrode/electrolyte, and no ion exchanges take place among the electrode as well as the electrolyte. This indicates that at the time of charging or discharging processes the electrolyte concentration remains constant. Through this procedure, the energy is stored in the EDLC [5]. Mainly carbonaceous materials such as carbon nanotubes (both multi-walled carbon nanotubes and single-walled

carbon nanotubes), graphene, carbon aerogels, activated carbon, carbon nanohorns etc. show the EDLC type of behavior. However, the individual material suffers from good capacitance properties. Though, their cyclic stability is relatively very high as compared to the pseudocapacitor material.

Over the last few decades, different types of carbonaceous materials have been broadly studied as the electrode materials for EDLC [28–31]. It is reported that the activated carbon having a large BET surface area of 500–3000 m^2/g has already been utilized in commercialized EDLC [31]. For any EDLC, the electrolyte is the main key factor to determine the capacitance properties. It is also reported that the double layer capacitance of any carbonaceous materials in organic electrolytes is much lesser than that in aqueous electrolytes. The occurrence of such behavior is due to the high resistance of the organic electrolytes [3]. Though, the operating voltage in aqueous electrolyte is much lesser (hardly about 1 V) because of the limitation of the electrochemical water decomposition, while it can be enhanced in organic electrolyte to above 2.0 V and in ionic liquid electrolyte to far beyond 3.0 V [32, 33]. A schematic representation of an electrochemical double layer capacitor is represented in Fig. 2b.

2.3 Hybrid Capacitor

Another type of supercapacitor is the hybrid supercapacitor that has asymmetrical electrode configuration in which one electrode consists of pseudocapacitor (redox active) materials whereas the second electrode consists of EDLC (carbonaceous) materials. Presently, these types of hybrid supercapacitors are extensively studied to take advantage of both the electrode materials in enhancing the energy density, power density and the overall cell voltages [34–36]. In this type of hybrid supercapacitor, both the faradaic capacitance and electrochemical double layer capacitance are taking place at the same time, in which one of them plays a major role. In both types of mechanisms, huge surface area, high conductivity as well as suitable pore size distribution are the main crucial properties of the electrode materials to reach excellent specific capacitance. Apart from asymmetric electrode configuration, these types of hybrid supercapacitor also can be fabricated by the help of pseudocapacitor as well as EDLC materials in an individual composite. As we know that the EDLC materials suffer from good specific capacitance but they have the advantages of excellent cyclic stability whereas, the pseudocapacitor material suffers from good cyclic stability although they achieve excellent specific capacitance. So, the combination of two *i.e.* pseudocapacitor materials along with EDLC materials to make a hybrid composite which serves the purpose fruitfully, that means the achievement of superior specific capacitance along with excellent cyclic stability [37–40].

3 Electrospinning

Electrospinning has been recognized for almost a century, and is regarded as a variation of the electrospray process [41–44]. At the time of electrospraying techniques, the liquid drop enlarges with an enhanced electric field. While the repulsive force induced by the distribution of charge on the surface of the drop is equalized by the surface tension of the liquid, the liquid drops deforms into a conical shape. A jet of liquid ejects from the cone tip, once the repulsive force surpasses the surface tension. In the case of low viscous liquids, the small droplets form as a result of the varicose breakup of the jet. When this behavior is applied in case of polymer solutions, instead of breaking up into single drops a solid fiber is produced.

The foremost observation on electrospinning, initially known as electrospraying was studied by Rayleigh in the year 1897 and Zeleny in the year 1914 [45]. Later, in the year 1934, a patent was published by Formhals in which the first explanation of an apparatus for the electrospinning process was demonstrated. The production of textile yarn from cellulose acetate was also described in that patent [46]. Though until the early 1990s, he did not receive much attention on that. From that time, various researches were carried out in order to assemble fiber processing by the help of electrostatic forces. Afterward, in the year 1969, Taylor was studied on electrically driven jets which happen to have a strong foundation in understanding the electrospinning technique. The electrospinning term was first used in the year around 1994. Later, an enormous contribution with this electrospinning technique was made by Reneker and co-workers [47–50]. They have mainly studied the electrospinning technique for a series of different polymers in their work. The mechanism for the development of polymer fibers throughout the electrospinning technique has been demonstrated by them. In order to increase its production as well as efficiency in fabricating versatile nanofibers, the electrospinning technique has undergone many modifications and improvements nowadays. There are numerous advanced methods and setups of electrospinning machines utilized totally according to the desired characterizations.

3.1 Fundamental of Electrospinning

Electrospinning is relatively very simple, inexpensive as well as a highly adaptable way to produce polymeric nanomaterials having diameter in the range of nanometers under a high electric field [51–53]. Apart from polymeric nanomaterials, inorganic nanomaterials along with one dimensional (1D) nanocomposite can also be produced by simply adding extra ingredients into the electrospun polymeric solution or combining with post-treatment procedures. Usually, a high-voltage power supply, a spinneret (generally syringe with built-up needle) and a grounded collector are the three major components for the basic laboratory electrospinning equipment. The high-voltage power supply provides a high voltage (several tens of kilovolts) which is applied among the spinneret as well as the collector. The pendent drop of the polymer

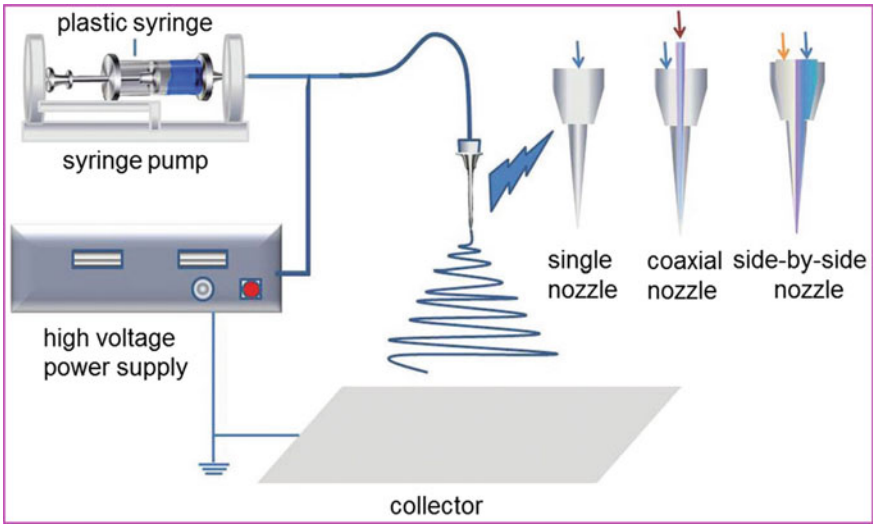

Fig. 3 Schematic diagram of the general laboratory setup for electrospinning with three different types of the nozzles. Reproduced from Ref. [54]

melt or solution is electrified and experiences the electrostatic forces under a high electric field and forms a droplet having conical shape (also known as Taylor cone) at the tip of the spinneret. When the strength of the electric field attains a critical value that means electrostatic force defeats the surface tension, a liquid jet of polymer melt or solution will eject and elongate from the tip of the Taylor cone, moving toward the electrode of the counter electrode. Then the charged jet experiences an unstable as well as whipping procedure, followed by the evaporation of the solvent or the solidification of the melt and the development of endless solid nanofibers on the counter collector. Generally, the spinneret is a syringe having a needle and utilizes as one of the electrodes of the electrospinning system. The inner diameter of a spinneret is in between 100 μm and 1 mm. A syringe pump is required to supply a controlled and constant rate to force the polymer solution to be fed through the spinneret. On the other hand, the polymer solution could be restricted in a glass tube by one end a of small diameter, otherwise a syringe without the push rod. Afterward, the syringe or the glass tube is tilted to generate the polymer solution flowing because of the gravity. A schematic diagram of the general laboratory setup for electrospinning as well as three different types of the nozzles has been highlighted in Fig. 3.

3.2 Fabrication Techniques of 3D Graphene Architectures

For the past few years, significant attention has been given to the development of 3D graphene materials with diverse morphologies and functionalities. It is observed that

the 3D graphene architectures have been developed by different synthetic procedures such as, assembly of graphene oxide (GO) sheets, self-assembly technique, template assisted technique, electrospinning techniques, as well as via direct deposition of 3D graphene structures through chemical vapor deposition (CVD).

Assembly Technique For the construction of 3D graphene architectures, assembly technique is one of the most promising approaches due to its benefits comprising low-cost, high yield along with simple functionalization of graphene. In this method, instead of graphene mainly GO solution is chosen because it acts as an amphiphilic material having hydrophilic edges along with a hydrophobic basal plane. For this reason, it can smoothly produce a stable dispersion in aqueous solutions. In order to get 3D graphene architectures, the GO sheets have to be reduced via thermal annealing or via chemical routes to reduced graphene oxide (rGO) at the last step of the assembly technique. The interactions such as hydrogen bonding, electrostatic interactions, van der Waals forces, dipole interactions as well as $\pi-\pi$ stacking are the main driving forces for the development of the 3D graphene architectures using assembly technique [55, 56].

Self Assembly Technique Another method for the fabrication of the 3D graphene is the self-assembly technique. In this technique mainly the 2D graphene sheets have been converted to 3D graphene architectures through different functionalities. Generally, via gelation of GO dispersion followed by reduction of GO to rGO, the 3D graphene architecture has been developed. Alternatively, by the help of hydrothermal or chemical reduction procedures the 3D graphene architectures can also be directly achieved through the self-assembly of GO sheets [57]. In these procedures, the GO sheets are easily self-assembled to form 3D architectures, and simultaneously reduced to rGO.

Template Assisted Technique Template assisted method is another suitable and feasible technique for the fabrication of 3D graphene architectures. In which pre-designed 3D templates like polystyrene, silicon dioxide has been used and after the reduction of GO it removes from the structures. Normally, the used template is bounded by graphene sheets because of the electrostatic interaction among positively charged templates as well as negatively charged graphene sheets. In this procedure more controlled morphologies and properties have been obtained. It is also observed that the size of the 3D graphene architectures directly depends on the template size. Up to now, considerable effort has already been given for the development of the 3D graphene architectures by the help of this template assisted technique [58, 59]. The 3D graphene architectures have also fabricated in another convenient method in which the assembly of GO sheets on top of the 3D templates followed by reduction of GO to rGO [57].

Electrospraying Technique The 3D graphene architectures have also been fabricated by the help of electrospinning or electrospraying techniques. Generally, the core–shell electrospinning techniques has attained great research interest because of its feasibility to achieve multi-functionality and use various materials in one step

procedure simply via removing deposition steps as like self assemble as well as template assisted method and therefore it extends the prospective applications in various fields like in energy storage, nanocomposites, drug delivery, sensors etc. [60]. Poudeh et al. fabricated the 3D graphene based hollow architectures via electrospraying technique [60]. In their study, 2D GO sheets are converted into 3D hollow and filled microspheres by the help of three different polymers [polystyrene (PS), polymethyl methacrylate (PMMA), and polyacrylonitrile (PAN)] through one step core–shell electrospraying method without applying any post treatment. It has been observed that the electrospraying technique prevents the aggregations and crumbling of graphene sheets by constructing 3D interconnected framework, and gives a homogeneous dispersion of graphene sheets in polymer solution under electric field, and permits the polymer chains to crawl into graphene layers forming intercalated structure. By taking the help of Mark-Houwink-Sakurada equation, the solution viscosities as well as the proper polymer concentration are determined to fabricate an ideal graphene based polymeric sphere structure through electrospraying. They have confirmed that the PS and PMMA are utilized as carrier polymers to convert 2D graphene sheets into 3D spheres because these polymers are easily processable for bead formation and are extensively utilized as templates to construct hollow 3D structures. The schematic representation of the fabrication of graphene-based 3D spheres by tri-axial electrospraying technique has been illustrated in Fig. 4.

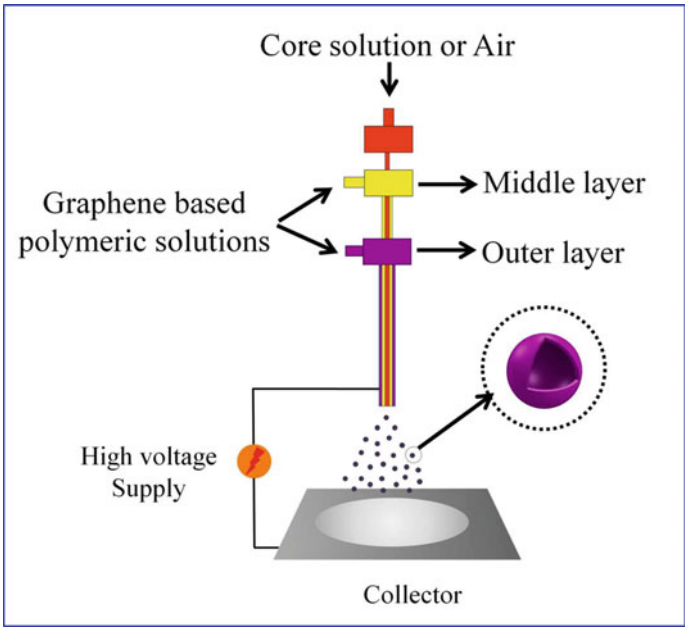

Fig. 4 Schematic illustration of the fabrication of graphene-based 3D spheres by tri-axial electrospraying technique. Reproduced from Ref. [60]

4 3D Graphene Nanocomposite for Supercapacitor

This section has been elaborately discussed about the fabrication 3D graphene-based nanocomposite by electrospinning techniques for the electrode materials for supercapacitors. Poudeh et al. successfully fabricated the platinum (Pt) – decorated 3D graphene-based carbon composite foam for the first time via core–shell electrospinning techniques instead of CVD methods [61]. In this procedure, by tailoring the concentration of polymer, applied voltage as well as polymer molecular weight, the multilayer graphene sheets are transformed into three different forms such as fiber, spheres and foam. When the polymer concentration is enhanced, it continues the generation of fibers, whereas, upon decreasing the concentration of polymer has caused the formation of graphene-based foam. Further, the reduction in molecular weight of polymer in electrospun solution has led to the construction of 3D spherical structures. All the structures 3D graphene-based spheres, foams as well as fibers have been confirmed from the morphological analysis. SEM images of electrosprayed, reduced and carbonized Pt-decorated 3D graphene-based foams as well as spheres are illustrated in Fig. 5. The electrochemical characteristic of the Pt-decorated 3D graphene-based structures has been investigated by cyclic voltammogram (CV) with the help of three-electrode method using 0.5 M H_2SO_4 as electrolyte, using Ag/AgCl as reference and platinum wire as reference electrode. The specific capacitance value was calculated from the cyclic voltammogram (CV) analysis. The Pt-decorated 3D graphene-based spheres exhibit the specific capacitance of 118 F/g at 1 mV/s scan rate, highest as compared to foam (54 F/g) and fiber (8 F/g). Actually, the 3D graphene

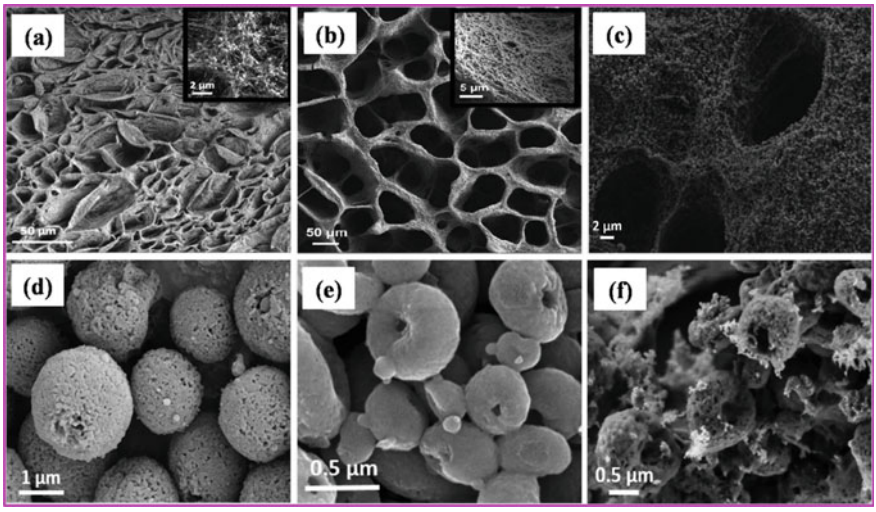

Fig. 5 SEM images of **a** electrosprayed, **b** reduced, and **c** carbonized Pt-decorated 3D graphene foam; SEM images of **d** electrosprayed, **e** reduced, and **f** carbonized Pt-decorated 3D graphene spheres. Reproduced from Ref. [61]

structures consist of micro and macro interconnected pores, which produces high surface area along with fast ion/electron transport channels. As the diameter of the Pt-nanoparticles is considerably high (~50 nm), hence the electrochemical behavior of Pt-decorated 3D graphene-based foam decreases, even if it has a unique structure. In the case of 3D graphene-based sphere, Pt-nanoparticles size decreased to 5 nm and the structure became more porous, thus improving the electrochemical properties. Their CV curves as well as GCD profile have been depicted in Fig. 6. It was observed that at low scan rate the CV curves are rectangular in shape indicating EDLC behavior, whereas the rectangular shape starts to distort on enhancing the scan rate up to 100 mV/s. Further, it has been observed from GCD profile that the Pt-decorated 3D graphene-based spheres reveal much higher discharge time compared to other structures indicating the better specific capacitance. Later the cyclic stability has been studied for all the three structures and the 3D graphene-based spheres retain their 88% of specific capacitance after 1000 charge–discharge cycles, while the foam and fibers maintain their 94 and 90% capacitance after the same charge–discharge cycles. The small diminish in cyclic stability of spheres stems from a rapid shrinking of pores of spheres because of their 3D structure, which effects in a decrease in the capacitance as time passes.

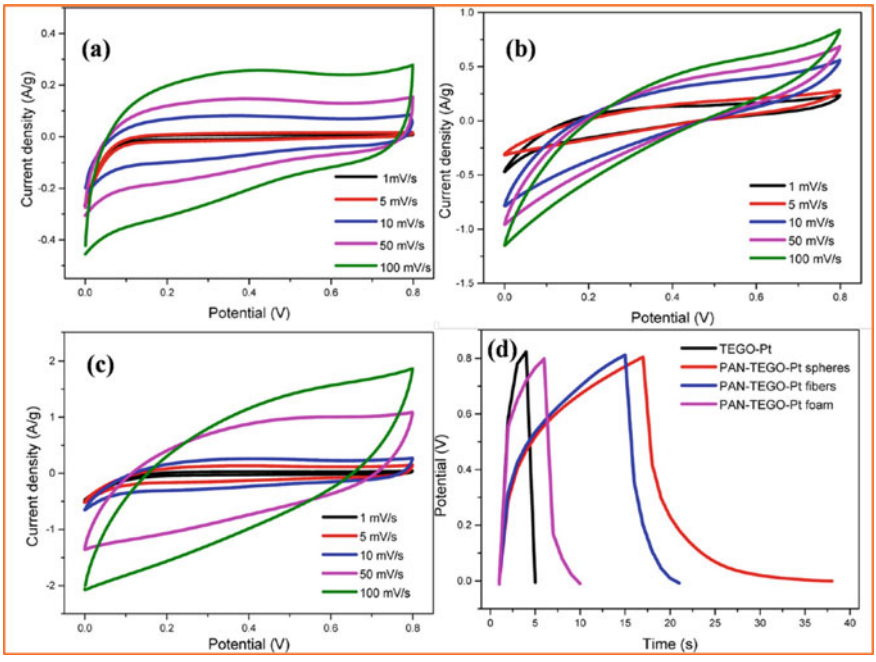

Fig. 6 CV curves at different scan rates for **a** fibers, **b** foam, **c** spheres, along with **d** GCD profiles at a 2 A/g current density for the Pt-decorated 3D graphene-based structures. Reproduced from Ref. [61]

The same groups have also fabricated the 3D urchin-shaped hybrid composite electrodes with PANI coated graphene and manganese oxide (Mn_3O_4) embedded in carbon fiber (CF) via core shell electrospinning, heat treatment followed by *in-situ* polymerization technique [62]. The electrospinning process was performed with an applied voltage of 12 kV, flow rate of 9 μL/min and having the nozzle to collector distance of 10 cm while atmospheric air was utilized as core material. Morphological analysis confirms the formation of 3D urchin-shaped PANI/Mn_3O_4/Graphene nanoplatelet (GNP) composite. The electrochemical performances were carried out by the help of a three-electrode system using 1 M H_2SO_4 as aqueous electrolyte. It has been observed that the 3D urchin-shaped PANI coated Mn_3O_4/GNP-CF composite produces the highest specific capacitance of 452 F/g at 1 mV/s scan rate and also retain their 89% of specific capacitance after 1000 charge–discharge cycles. The introduction of GNP into the fiber structures helped both ions along with electron transport and gave highly electroactive sites that shortened the diffusion paths by bridging the adjacent individual PANI chains.

Further, Huang et al. reported an efficient surface-induced co-assembly strategy for the novel design and reconstruction of electrospun nanofibers into 3D graphene/carbon nanofiber (CNF) composite aerogels [GCA] having hierarchical structures for the efficient energy storage material [63]. The preparation pathway of 3D GCA structures through co-assembly followed by carbonization technique has been schematically illustrated in Fig. 7a. Where, the 2D graphene nanosheets act as cross-linker and the 1D electrospun CNF networks serve as the rigid skeleton. A direct comparison among GO/oPAN aerogels with 3D GCA in Fig. 7b manifests that the GCA perfectly retain the integrated 3D structure of GO/oPAN aerogels, signifying the feasible protocol for the synthesis of electrospun nanofiber-based all-carbon aerogels. It has been also observed that the 3D GCA monolith can easily stand on a soft hair of dog's tail grass (*Setaria viridis*), shown in Fig. 7c. Further, it is illustrated that the 3D GCA can totally recover its original shape without any mechanical fracture after ~70% of compression, shown in Fig. 7d. From the morphological analysis it has been observed that the GCA exhibits an interconnected, porous 3D framework with continuous macropores ranging from 100 nm to 10 μm, in which short CNFs serving as rigid skeletons are intertwined in random directions while large graphene flakes act as cross-linkers and bridge the CNF ribs to form an integrated network, shown in Fig. 7e. The inset of Fig. 7e specifies the veins of CNFs ribs by red dots, revealing that CNFs are bridged to form connected pathways which will further improve the structural stability of GCA. The combination of hierarchical 3D structures having numerous macropores, with high ion-accessible surface area of 57.8 m^2/g and interconnected electrically conductive network creates GCA extremely desirable for electrochemical behaviors. They have performed the electrochemical characteristics by a three-electrode system using 6 M KOH aqueous electrolyte. The CV curves of the 3D GCA structures show nearly rectangular in shape signifying a typical EDLC behavior and fast charging/discharging processes, shown in Fig. 8a. Figure 8b represents the GCD plots at various current densities of the 3D GCA structures and conformed longer galvanostatic charge–discharge time as compared to CNFs. It has been observed that the 3D GCA structures exhibited the highest

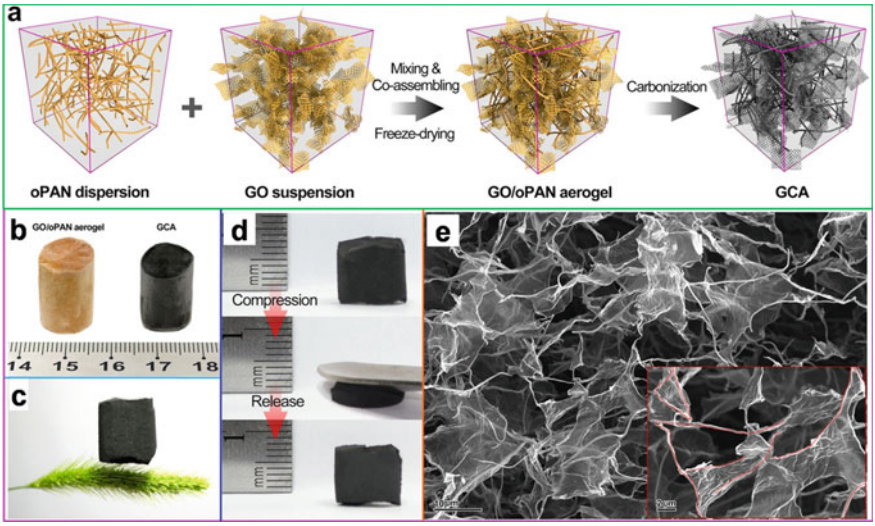

Fig. 7 **a** Schematic representation of the preparation pathway of the 3D GCA structure by co-assembly and carbonization; demonstration on the structural stability and elasticity of GCA with low density, and characterization on the interconnections among graphene and CNF with GCA: **b** GCA maintains the good cylindrical shape of GO-oPAN aerogels without noticeable shrinkage, **c** a GCA cylinder standing on the soft hair of dog's tail grass (*Setaria viridis*), and **d** GCA aerogel can recover its original shape after a strong compression. **e** SEM image of the microscopically porous architecture of GCA, with the inset showing the CNF framework by red dots. Reproduced from Ref. [63]

specific capacitance of 180 F/g at 1 A/g current density, much higher as compared to CNFs (76 F/g at A/g). The specific capacitance values at different current densities are summarized in Fig. 8c. Later, the cyclic stability analysis was carried out and it was observed that the 3D GCA structures retained their 94.8% of specific capacitance after 2000 charge–discharge cycles, shown in Fig. 8d.

An activated carbon nanowhisker (ACNWs) wrapped-on graphitized electrospun nanofiber (GENF) network [ACNWs/GENFN] having 3D porous structures was prepared by the help of electrospinning techniques followed by in-situ polymerization as a new type of binder-free electrode materials for supercapacitors was studied by He et al. [64]. The digital images of the as prepared GENF mat (gray in color) along with PANI/GENF mat (green in color) are shown in Fig. 9a. From the morphological analysis it was observed that a kind of highly porous 3D network material composited by a large amount of GENFs with smooth surface having diameter of 450–600 nm, illustrated in Fig. 9b and the inset of Fig. 9b displayed an ordered graphitic structure, which implied a high electrical conductivity. The green color mat was achieved after the growth of a layer of ordered needle-like PANI nanowhiskers (PANI-NWs) on the GENFs. Figure 9c exhibited the SEM images of 3D PANI-NWs/GENF composite fibers and observed a coaxial structure having an outer diameter of about 1.2 μm and length of about 300 nm. When the PANI-NWs are being treated at high temperature

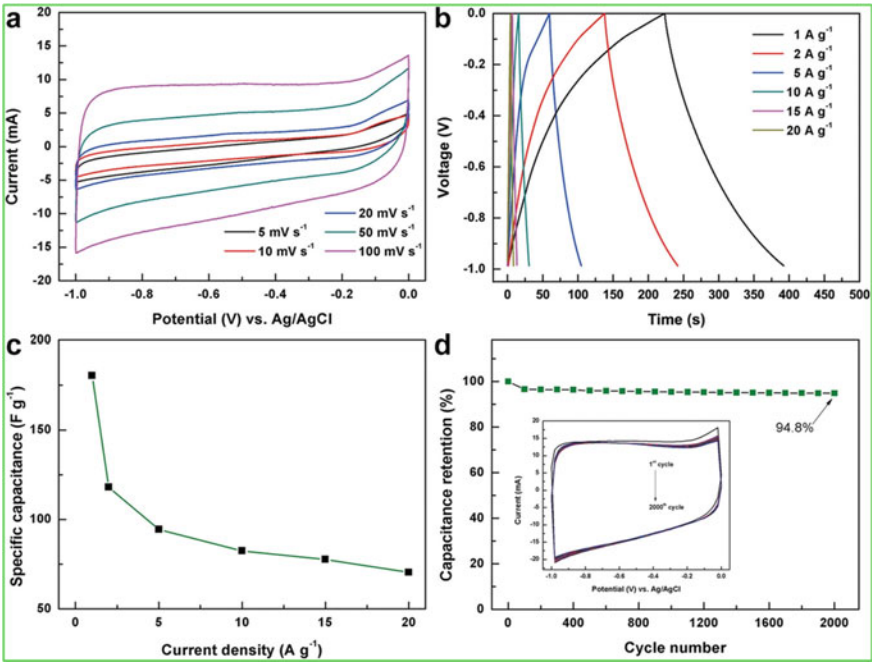

Fig. 8 Capacitive tents for 3D GCA electrodes: **a** CV curves at different scan rates, **b** GCD curve at various current densities, **c** specific capacitance at different current densities, and **d** cyclic stability test up to 2000 charge–discharge cycles, with inset showing the CV curve of the 1st cycle and CV curves of the 2000 cycles. Reproduced from Ref. [63]

it is converted to carbon nanowhiskers (CNWs), shown in Fig. 9d. Further increase in the carbonization temperature, the CNWs on the surface of GENFs become sparser and blunter, illustrated in Fig. 9e. The electrochemical performances were carried out in a three-electrode measurement system using 6 M KOH solution as electrolyte. The 3D coaxial ACNWs/GENF network composite exhibited the highest specific capacitance of 176.5 F/g at a current density of 800 A/g, ultrahigh power density of 250 kW/kg and good cyclic stability without any capacitance decreases even after 10,000 charge/discharge cycles at 100 A/g. Such a good rate capacitance performance of the ACNWs/GENFN was attributed to the 3D porous architecture, high electrically conductive network of GENFN and high utilization rate of porous ACNWs.

In another study, 3D interconnected networks of reduced graphene oxide (rGO)/thorn-like TiO_2 nanofiber (TTF) aerogels [GTTF aerogels] having different TTF weight ratios were successfully prepared by electrospinning, silica etching followed by hydrothermal combination technique [65]. From the morphological analysis of the GTTF-20 aerogels it was confirmed that the interconnected porous 3D structure has a pore diameter of several micrometers. Later, all the electrochemical tests were performed by the help of a three-electrode cell using 1 M Na_2SO_4 as the electrolyte. The working electrode has been fabricated by directly placing a small

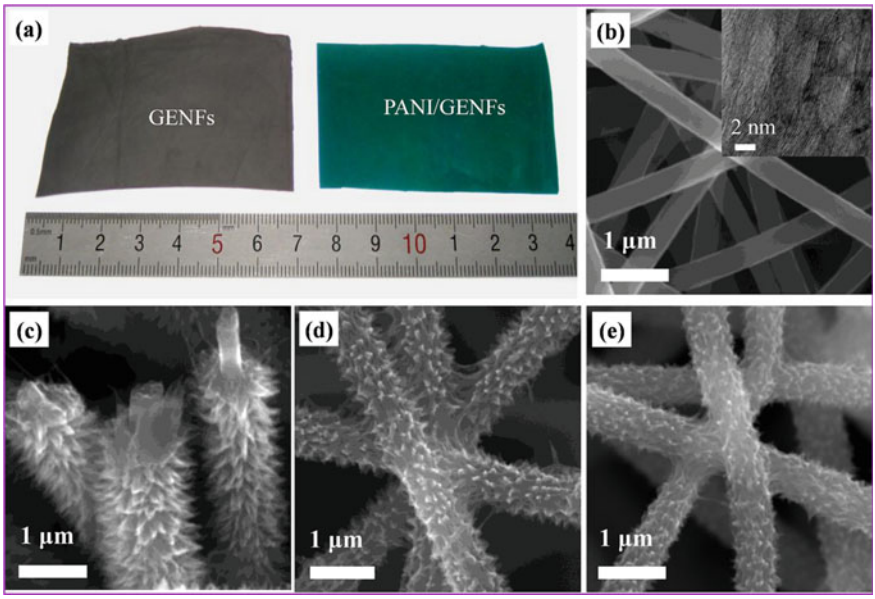

Fig. 9 **a** Digital images of GENF mat (gray) and PANI/GENFs mat (green), **b** SEM images of GENFs, inset TEM image of GENFs, **c** PANI-NWs/GENFs, **d** C700 [CNWs/GENFs carbonized at 700 °C], **e** AC-700-600 [sample C700 activated at 600 °C]. Reproduced from Ref. [64]

piece of aerogels (~10 mm in diameter and ~1.5 mm in height) among two pieces of nickel foam (with 3 cm^2 in area) without any additives followed by pressing at 10 MPa to make the electrode materials adhere to the current collector more completely. From the GCD curve it was examined that the curves are linear and symmetrical in nature over the entire potential range, depicted in Fig. 10a. Their triangular shape also indicates excellent capacitive behavior. The GCD curve of the 3D interconnected structure based GTTF-20 aerogels at different current densities (1–5 A/g) has been illustrated in Fig. 10b. Figure 10c showed the obtained specific capacitance values at various current densities for the GTTF based 3D structures. The 3D interconnected structure based GTTF-20 aerogels exhibited the highest specific capacitance of 178 F/g at a 1 A/g current density and also maintain their 90.3% of specific capacitance after 3000 charge discharge cycles at a current density of 5 A/g, Fig. 10d. Inset of Fig. 10d showed GCD curve of the 1st as well as the 3000th cycle.

So, up to this it was seen that the development of 3D graphene-based architectures by the help of electrospinning techniques followed by other techniques tremendously enhances the ion-accessible surface area and thereby significantly improves the electrochemical characteristics. It was also observed that some of the graphene-based nanocomposites fabricated via electrospinning techniques considered as the superior electrode materials for supercapacitors. Like, Tai et al. fabricated a flexible and freestanding carbon nanofiber/graphene nanosheet (CNF/GNS) composite paper by the help of electrospinning technique followed by high-temperature annealing using

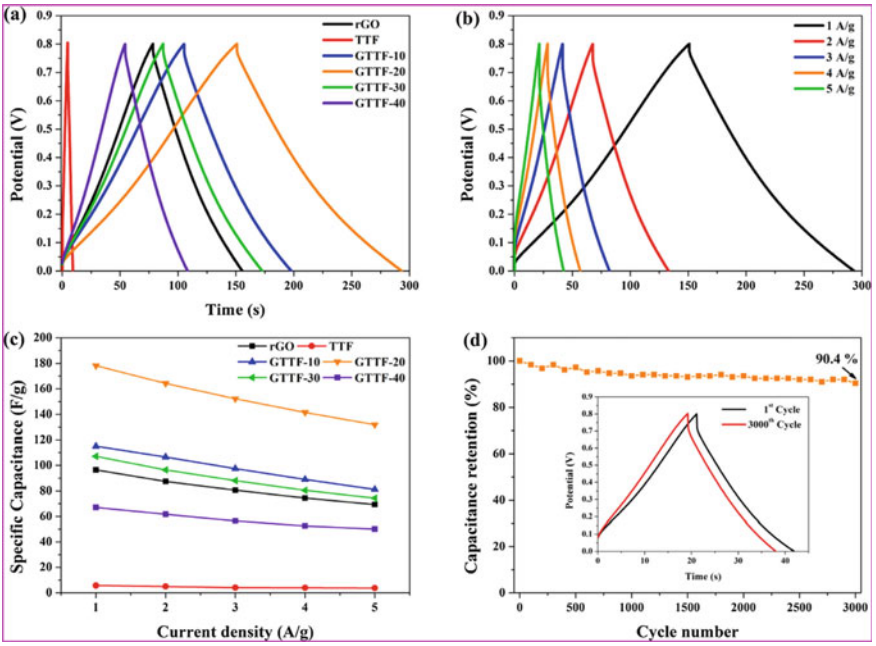

Fig. 10 **a** GCD curves of 3D GTTF aerogel-based electrodes at a current density of 1 A/g, **b** GCD curves of the GTTF-20 electrode at different current densities, **c** comparative specific capacitances of rGO and 3D GTTF aerogels, and **d** cycle performance of the 3D GTTF-20 electrode. Reproduced from Ref. [65]

a polyacrylonitrile/GNS/dimethylformamide mixture as electrospun precursor [66]. The as fabricated CNF/GNS paper showed excellent specific surface area of 447 m^2/g and an average pore size of 8.16 nm along with superior electrical conductivity of 200 S/cm. The electrochemical properties of the paper like freestanding CNT/GNS composites were carried out by the help of a three-electrode system in 6 M KOH electrolyte at room temperature. The as fabricated freestanding CNF/GNS paper achieved the highest specific capacitance of 197 F/g at a 1.25 A/g current density which is about 24% higher as compared to the pure CNF paper. The composite paper also retains its 84% of specific capacitance after 1500 charge–discharge cycles.

In another study, electrospun carbon nanofiber/graphene (CNF/G) composite was prepared by the help of *in-situ* electrospinning polymeric nanofibers with simultaneous spraying of graphene oxide, followed by heat treatment [67]. It was observed that the freestanding CNF web acts as a framework for sustaining graphene, which helps to prevent the agglomeration of graphene and to provide a high conductivity for the efficient charge transfer to the pores. The electrochemical measurements were carried out in a three-electrode electrochemical cell using 6 M KOH as electrolyte at 25 °C. The CNF/G composite achieved the highest specific capacitance of 183 F/g at a 1 A/g current density which is approximately 1.6 times high as compared to the pristine CNF. The greater specific capacitance can be attributed

not only to large channels among graphene and CNF, which functions as reservoir for more electrolyte throughout the charging-discharging process, but also to large pores in the CNF/G composite, which accelerate the ionic transportation in pores. Later, the cyclic stability tests were performed at 1 A/g current density and it was observed that the CNF/G composite maintained their 92% of specific capacitance after 4500 charge–discharge cycles. Further, a nanocomposite having the combination of graphene nanoplatelets and carbon nanofibers were successfully fabricated by using a one-step solution based on the electrospinning technique for the potential electrode materials for supercapacitor [68]. The electrochemical performances were evaluated using two-electrode configuration in which liquid electrolyte socked nylon membrane filter was sandwiched between the prepared samples before being tightly fitted into an electrochemical cell. The as mentioned nanocomposite exhibited the specific capacitance of 86.11 F/g as well as retained their 90% of capacitance even after 1000 charge–discharge cycles.

In another work, the graphene oxide/polyaniline/polyvinylidene fluoride (GO/PANI/PVDF) composite nanofiber was fabricated by the help of electrospinning techniques as the electrode materials for supercapacitors reported by Rose et al. [69]. The electrochemical characteristics were performed at room temperature in a three-electrode set up using 1 M H_2SO_4 as electrolyte. The specific capacitance value was calculated by the help of CV curve and it was observed that the GO based composite nanofiber achieved the highest specific capacitance of 170.63 F/g, energy density of 13.92 W/kg, and density of 316.36 W/kg, respectively. The same research group also developed the GO/PANI/PVA composite nanofiber via electrospinning process for the supercapacitor electrode materials [70]. Here, all the parameters for the electrochemical characterization remain the same. The composite nanofiber reached the specific capacitance of 438.8 F/g. It was also reported that the development of flexible all-solid-state supercapacitor based on free standing, binder-free carbon nanofiber@polypyrrole@graphene (CNTs@PPy@rGO) core-double-shell film fabricated by carbonization of electrospun PAN nanofiber network followed by electrochemical deposition of PPy and then rGO layer coating [71]. The electrochemical measurements for the all-solid-state flexible supercapacitor were carried out by two-electrode setup using PVA/H_3PO_4 gel electrolyte. It was observed that the flexible all-solid-state supercapacitor device showed the highest specific capacitance of 188 F/g at the scan rate of a 2 mV/s and also retained their 59.5% of specific capacitance after 10,000 consecutive charge–discharge cycles. In order to better understand the underlying mechanism behind the excellent electrochemical characteristics of the all-solid-state flexible supercapacitor, the electrochemical performance of the CNFs@PPy@rGO electrode was further evaluated in three-electrode setup using 3 M KCl solution as aqueous electrolyte. In this case the core-double-shell electrode achieved the specific capacitance of 336.2 F/g at the scan rate of a 2 mV/s and also holds 98% of capacitance after 2500 charge–discharge cycles. Further, the GO reinforced electrospun CNF was developed for the ultrathin supercapacitor electrode [72]. Upon the addition of functionalized GO into a polymeric solution and subjected to an electrospinning technique, non-woven random nanofiber embedded with GO

sheets was obtained. Their electrochemical properties were evaluated via a two-electrode system using 6 M KOH as electrolyte. The mentioned composite electrode showed the specific capacitance of 140.10 F/g at a 1 A/g current density and also retained their 96.2% of specific capacitance after vigorous 1000 charge–discharge cycles. In another study, graphene-beaded CNF (G/CNF) electrode was prepared by electrospinning PAN/N,N-dimethylformamide (DMF) solution dispersed with oxidized graphene nanosheets, followed by carbonization at 800 °C inside the tubular quartz furnace as the superior electrode materials for supercapacitor [73]. In this case, the electrochemical characterization was performed in a two-electrode system utilizing 6 M KOH as electrolyte. The G/CNF electrode researched the specific capacitance of 263.7 F/g at a 100 mA/g current density and also retained its 86.9% of specific capacitance after 2000 charge–discharge cycles.

Qiu et al. synthesized nitrogen-doped active carbon fiber/reduced graphene oxide (ACF-rGO-N) nanocomposite by electrospinning, calcinations, self-assemble reduction in addition to post treatment nitrogen doping procedure [74]. From the morphological analysis it was observed that the rGO nanosheets are not only dispersed homogeneously on the surface of the ACF, but also embedded into the ACF framework, forming the line-plane structure with the non-covalent bonding. It was also examined that the N-doping post treatment has no significant effect on the morphology of ACF-rGO. Initially, the electrochemical performance was measured in a three-electrode system in which both acidic (1 M H_2SO_4) and basic (6 M KOH) electrolytes were utilized. Later, it was studied in a quasi-solid state two-electrode system in which PVA/KOH gel electrolyte has been used which also acted as a separator for the solid-state device. It was reported that the in 6 M KOH electrolyte the ACF-rGO-N nanocomposite exhibited the highest specific capacitance of 283 F/g at 0.2 A/g current density, whereas in 1 M H_2SO_4 the nanocomposite achieved the specific capacitance of 301 F/g at the same current density. The cyclic stability of the ACF-rGO-N nanocomposite was further studied in two different electrolytes and observed that capacitance retention of 98% in 6 M KOH and 96% in 1 M H_2SO_4 electrolyte after consecutive 1000 charge–discharge cycles. Afterword, the solid-state symmetric supercapacitor device was characterized and it was observed from CV curves that there were no significant redox peaks at various scan rates indicating the typical double-layer capacitive behavior, shown in Fig. 11a. From the GCD curves it was noticed the isosceles triangles at different current densities with no distinct voltage drop, illustrated in Fig. 11b. The solid-tate symmetric device achieved the high specific capacitance of 254 F/g at a 0.2 A/g current density. The specific capacitance values at different current densities are represented in Fig. 11c. The symmetrical supercapacitor also exhibited the energy density of 35.2 Wh/kg as well as power density of 399.1 W/kg at a 0.2 A/g current density. Lastly, the symmetric supercapacitor also achieved excellent cyclic stability with 99% capacitance retention after 10,000 charge–discharge cycles, shown in Fig. 11d.

Similarly, by the help of electrospinning technique the GO/vanadium pentoxide (V_2O_5) nanofiber was prepared for the supercapacitor electrode materials [75]. Lastly, it was annealed at 550 °C to get the final composite. The electrochemical behaviors were carried out in a three-electrode cell setup using two aqueous electrolytes of

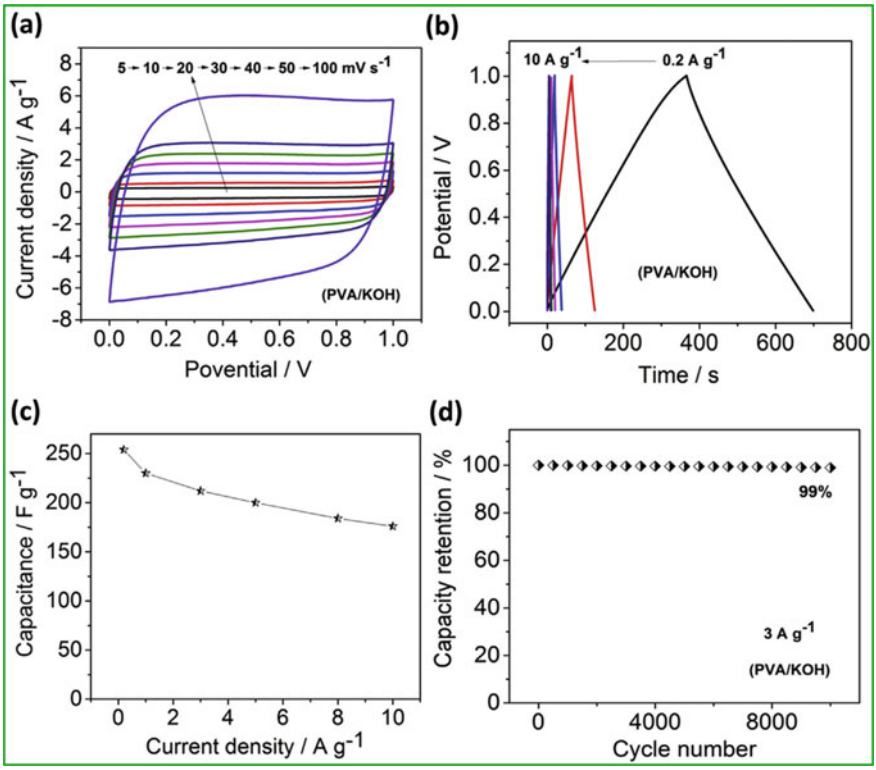

Fig. 11 Electrochemical performances of the ACF-rGO-N based solid state symmetric supercapacitor: **a** CV curved at various scan rates, **b** GCD curves different current densities, **c** specific capacitance values at various current densities, **d** cycling stability plots at current densities of 3 A/g. Reproduced from Ref. [74]

2 M KOH and 1 M H_2SO_4. The annealed GO based electrospun nanofiber exhibited the highest specific capacitance of 453.824 F/g at the scan rate of 10 mV/s in 2 M KOH electrolyte. In another study, composite of MnO_2 decorated on hierarchical porous carbon nanofiber/graphene (MnO_2/HPCNF/G) have been fruitfully fabricated via one-step electrospinning technique followed by thermal treatment as superior electrode materials for electrochemical supercapacitor [76]. The electrochemical behaviors were studied in a two-electrode test using 6 M KOH electrolyte in which the two symmetric MnO_2/HPCNF/G composite electrode were directly utilized as electrode without any polymer binder. The MnO_2/HPCNF/G composite electrode exhibited the highest specific capacitance of 210 F/g at 1 mA/cm^2 current density. It has been also observed that the MnO_2/HPCNF/G composite electrode achieved the excellent energy density of 24 Wh/kg, high power density of 400 W/kg along with superior cyclic stability as it retained 95.7% of specific capacitance after 1000 charge–discharge cycles. So, comparatively all the literature that has highlighted the 3D graphene-based nanocomposites fabricated by the help of electrospinning

techniques for the electrode materials for supercapacitors has been discussed in this section.

5 Summary

This chapter has proposed the up to date research activities in the field of 3D graphene-based nanocomposites as well as graphene based related materials fabricated through electrospinning techniques for the efficient electrode materials for supercapacitors. The basic concept of supercapacitors along with their classifications, clear overview of electrospinning including the electrospinning process and the fabrication techniques of 3D graphene architectures has been systematically discussed. The literature related to the 3D graphene architectures-based nanocomposites via electrospinning process has been elaborately discussed including their morphological, electrochemical process parameter as well as their detailed experimental electrochemical results. It has been observed that the development of 3D architectures helps to improve the electrochemical characteristics. Though many research have already been done and also going on in the field of 3D graphene architectures based nanocomposites via electrospinning process for electrode materials but till further research is required to explore in this field basically on the fabrication of 3D graphene architectures through electrospinning techniques for supercapacitors in addition to the development of 3D graphene architectures based flexible as well as stretchable supercapacitor device for practical applications. Hope this chapter will help the beginners who are working in the particular field of 3D graphene-based nanocomposites by electrospinning techniques for the electrode materials for supercapacitors.

Acknowledgements S. Dhibar would like to thank Council of Scientific & Industrial Research (CSIR), Human Resource Development Group, New Delhi, India, for the CSIR Research Associate Fellowship [File No. 09/080(1105)/2019-EMR-I]. Dr. Malik acknowledges CSIR, INDIA (Project No. 01(2875)/17/EMR-II) for the financial support.

References

1. Liu, C., Li, F., Ma, L.P., Cheng, H.M.: Advanced materials for energy storage. Adv. Mater. **22**, E28–E62 (2010)
2. Winter, M., Brodd, R.J.: What are batteries, fuel cells and supercapacitors? Chem. Rev. **104**, 4245–4270 (2004)
3. Simon, P., Gogotsi, Y.: Materials for electrochemical capacitors. Nat. Mater.**7**, 845–854 (2008)
4. Service, R.F.: New 'supercapacitor' promises to pack more electrical punch. Science **313**, 902 (2006)
5. Wang, G., Zhang, L., Zhang, J.: A review of electrode materials for electrochemical supercapacitors. Chem. Soc. Rev. **41**, 797–828 (2012)
6. Miller, J.R., Simon, P.: Electrochemical capacitors for energy management. Science **321**, 651–652 (2008)

7. Gogotsi, Y., Presser, V.: Carbon Nanomaterials. CRC Press, Boca Raton, FL (2006)
8. Kumar, A., Deka, M.: Nanofiber reinforced composite polymer electrolyte membranes. InTech (2010)
9. Ramakrishna, S., Fujihara, K., Teo, W.-E., Lim, T.-C., Ma, Z.: An Introduction to Electrospinning and Nanofibers. World Scientific Publishing Co Pte Ltd., National University of Singapore (2005)
10. Jeong, J.S., Moon, J.S., Jeon, S.Y., Park, J.H., Alegaonkar, P.S., Yoo, J.B.: Mechanical properties of electrospun PVA/MWCNTs composite nanofibers. Thin Solid Films **515**, 5136–5141 (2007)
11. Almecija, D., Blond, D., Sader, J.E., Coleman, J.N., Boland, J.J.: Mechanical properties of individual electrospun polymer-nanotube composite nanofiber. Carbon **47**, 2253–2258 (2009)
12. Chen, S., He, S., Hou, H.: Electrospinning technology for applications in supercapacitors. Curr. Org. Chem. **17**, 1402–1410 (2013)
13. Cavaliere, S., Subianto, S., Savvch, I., Jones, D.J., Rozière, J.: Electrospinning: designed architectures for energy conversion and storage devices. Energ. Environ. Sci. **4**, 4761–4785 (2011)
14. Thavasi, V., Singh, G., Ramakrishna, S.: Electrospun nanofiber in energy and environmental applications. Energ. Environ. Sci. **1**, 205–221 (2008)
15. Dong, Z.X., Kennedy, S.J., Wu, Y.Q.: Electrospinning materials for energy-related applications and device. J. Power Sour. **196**, 4886–4904 (2011)
16. Qi, Z., Koenig, G.M.: Flow battery systems with solid electroactive materials. J. Vac. Sci. Technol. B **35**, 040801–040827 (2017)
17. Conway, B.E.: Electrochemical Supercapacitors. Kluwer Academic/Plenum Press, New York (1999)
18. Wu, M.S., Chiang, P.C.J.: Fabrication of nanostructured manganese oxide electrodes for electrochemical capacitors. Electrochem. Solid-State Lett. **7**, A123–A126 (2004)
19. Sugimoto, W., Iwata, H., Murakami, Y., Takasu, Y.: Electrochemical capacitor behavior of layered ruthenic acid hydrate. J. Electrochem. Soc. **151**, A1181–A1187 (2004)
20. Wu, M.-S., Lee, R.-H., Jow, J.-J., Yang, W.-D., Hsieh, C.-Y., Weng, B.-J.: Nanostructured iron oxide films prepared by electrochemical method for electrochemical capacitors. Electrochem. Solid-State Lett. **12**, A1–A4 (2009)
21. Meher, S.K., Rao, G.R.: Ultralayered Co_3O_4 for high performance supercapacitor applications. J. Phys. Chem. C **115**, 15646–15654 (2011)
22. Xia, X.-H., Tu, J.-P., Wang, X.-L., Gu, C.-D., Zhao, X.-B.: Mesoporous Co_3O_4 monolayer hollow-sphere array as electrochemical pseudocapacitor material. Chem. Commun. **47**, 5786–5788 (2011)
23. Shen, L., Yu, L., Wu, H.B., Yu, X.-Y., Zhang, X., Lou, X.W. (David).: Formation of nickel cobalt sulfide ball-in-ball hollow spheres with enhanced electrochemical pseudocapacitive properties. Nat. Commun. **6**, 6694 (2015)
24. Xiao, J., Wan, L., Yang, S., Xiao, F., Wang, S.: Design hierarchical electrodes with highly conductive $NiCo_2S_4$ nanotube arrays grown on carbon fiber paper for high-performance pseudocapacitors. Nano Lett. **14**, 831–838 (2014)
25. Huang, L., Chen, D., Ding, Y., Feng, S., Wang, Z.L., Liu, M.: Nickel–cobalt hydroxide nanosheets coated on $NiCo_2O_4$ nanowires grown on carbon fiber paper for high-performance pseudocapacitors. Nano Lett. **13**, 3135–3139 (2013)
26. Tomboc, G.M., Jadhav, H.S., Kim, H.: PVP assisted morphology-controlled synthesis of hierarchical mesoporous $ZnCo_2O_4$ nanoparticles for high-performance pseudocapacitor. Chem. Eng. J. **308**, 202–213 (2017)
27. Chen, X., Paul, R., Dai, L.: Carbon-based supercapacitors for efficient energy storage. Natl. Sci. Rev. **4**, 453–489 (2017)
28. Béguin, F., Presser, V., Balducci, A., Frackowiak, E.: Carbons and electrolytes for advanced supercapacitors. Adv. Mater. **26**, 2219–2251 (2014)
29. Frackowiak, E.: Carbon materials for supercapacitor applications. Phys. Chem. Chem. Phys. **9**, 1774–1185 (2007)

30. Pandolfo, A.G., Hollenkamp, A.F.: Carbon properties and their role in supercapacitors. J. Power Sour. **157**, 11–17 (2006)
31. Zhang, L.L., Zhao, X.S.: Carbon-based materials as supercapacitor electrodes. Chem. Soc. Rev. **38**, 2520–2531 (2009)
32. Fernandez, J.A., Arulepp, M., Leis, J., Stoeckli, F., Centeno, T.A.: EDLC performance of carbide-derived carbons in aprotic and acidic electrolytes. Electrochim. Acta **53**, 7111–7116 (2008)
33. Chen, R., Wu, F., Li, L., Xu, B., Qiu, X., Chen, S.: Novel binary room-temperature complex system based on LiTFSI and 2-oxazolidinone and its characterization as electrolyte. J. Phys. Chem. C **111**, 5184–5194 (2007)
34. Ma, S.-B., Nam, K.-W., Yoon, W.-S., Yang, X.-Q., Ahn, K.-Y., Oh, K.-H., Kim, K.-B.: A novel concept of hybrid capacitor based on manganese oxide materials. Electrochem. Commun. **9**, 2807–2811 (2007)
35. Zhou, Y., Lachman, N., Ghaffari, M., Xu, H., Bhattacharya, D., Fattahi, P., Abidian, M.R., Wu, S., Gleason, K.K., Wardle, B.L., Zhang, Q.M.: A high performance hybrid asymmetric supercapacitor *via* nano-scale morphology control of graphene, conducting polymer, and carbon nanotube electrodes. J. Mater. Chem. A **2**, 9964–9969 (2014)
36. Gao, Z., Song, N., Li, X.: Microstructural design of hybrid CoO@NiO and graphene nanoarchitectures for flexible high performance supercapacitors. J. Mater. Chem. A **3**, 14833–14844 (2015)
37. Sahoo, S., Dhibar, S., Hatui, G., Bhattacharya, P., Das, C.K.: Graphene/polypyrrole nanofiber nanocomposite as electrode material for electrochemical supercapacitor. Polymer **54**, 1033–1042 (2013)
38. Dhibar, S., Das, C.K.: Silver nanoparticles decorated polyaniline/multi-walled carbon nanotubes nanocomposite for high performance supercapacitor electrode. Ind. Eng. Chem. Res. **53**, 3495–3508 (2014)
39. Dhibar, S., Bhattacharya, P., Hatui, G., Sahoo, S., Das, C.K.: Transition metal doped polyaniline/single walled carbon nanotubes nanocomposite an efficient electrode material for high performance supercapacitor. ACS Sustain. Chem. Eng. **2**, 1114–1127 (2014)
40. Dhibar, S.: Electrochemical behaviour of graphene and carbon nanotubes based hybrid polymer composites. In: Thakur, V.K., Thakur, M.K., Gupta, R.K. (eds.) Hybrid Polymer Composite Materials: Processing, pp. 211–248. Woodland Publishing, United Kingdom (2017)
41. Rayleigh, L.: On the equilibrium of liquid conducting masses charged with electricity. Philos. Mag. **14**, 184–186 (1882)
42. Cooley, J.F.: Apparatus for electrically dispersing fluids. US patent 692,631 (1902)
43. Morton, W.J.: Methods of dispersing fluids. US patent 705,691 (1902)
44. Wilson, C.T.R., Taylor, G.I.: The bursting of soap-bubbles in a uniform electric filed. Proc. Camb. Phil. Soc. **22**, 728–730 (1925)
45. Bhardwaj, N., Kundu, S.C.: Electrospinning: a fascinating fiber fabrication technique. Biotechnol. Adv. **28**, 325–347 (2010)
46. Formhals, A.: Process and apparatus for preparing artificial threads. US Patent 1975504 (1934)
47. Doshi, J., Srinivasan, G., Reneker, D.: A novel electrospinning process. Polym. News **20**, 206–207 (1995)
48. Fang, X., Reneker, D.H.: DNA fibers by electrospinning. J. Macromol. Sci. Phys. B **36**, 169–173 (1997)
49. Fong, H., Reneker, D.H.: Elastomeric nanofibers by styrene-butadiene-styrene triblock copolymer. J. Polym. Sci. Part B Polym. Phys. **37**, 3488–3493 (1999)
50. Yarin, A.L., Koombhongse, S., Reneker, D.H.: Bending instability in electrospinning nanofibers. J. Appl. Phys. **89**, 3018–3026 (2001)
51. Greiner, A., Wendorff, J.H.: Electrospinning: a fascinating method for the preparation of ultrathin fibers. Angew. Chem., Int. Ed. **46**, 5670–5703 (2007)
52. Li, D., Xia, Y.: Electrospinning of nanofibers: reinventing the wheel? Adv. Mater. **16**, 1151–1170 (2004)

53. Lu, X., Wang, C., Wei, Y.: One-dimensional composite nanomaterials: synthesis by electrospinning and their applications. Small **5**, 2349–2370 (2009)
54. Lu, X., Wang, C., Favier, F., Pinna, N.: Electrospun nanomaterials for supercapacitor electrode: designed and architectures and electrochemical performance. Adv. Energ. Mater. **7**, 1601301 (2017)
55. Bai, H., Li, C., Wang, X., Shi, G.: On the gelation of graphene oxide. J. Phys. Chem. C **115**, 5545–5551 (2011)
56. Xu, Y., Sheng, K., Li, C., Shi, G.: Self-assembled graphene hydrogel via a one-step hydrothermal process. ACS Nano **4**, 4324–4330 (2010)
57. Cao, X., Yin, Z., Zhang, H.: Three-dimensional graphene materials: preparation, structures and application in supercapacitors. Energ. Environ. Sci. **7**, 1850–1865 (2014)
58. Zhang, J., Yu, Y., Liu, L., Wu, Y.: Graphene-hollow PPy sphere 3D-nanoarchitecture with enhanced electrochemical performance. Nanoscale **5**, 3052–3057 (2013)
59. Cai, D., Ding, L., Wang, S., Li, Z., Zhu, M., Wang, H.: Facile synthesis of ultrathin-shell graphene hollow spheres for high-performance lithium-ion batteries. Electrochim. Acta **139**, 96–103 (2014)
60. Poudeh, L.H., Okan, B.S., Zanjani, J.S.M., Yildiz, M., Menceloglu, Y.Z.: Design and fabrication of hollow and filled graphene-based polymeric spheres via core-shell electrospraying. RSC Adv. **5**, 91147–91157 (2015)
61. Poudeh, L.H., Letofsky-Papst, I., Cebeci, F.Ç., Menceloglu, Y., Yildiz, M., Okan, B.S.: Facile synthesis of single- and multi-layer graphene/Mn_3O_4 integrated 3D urchin-shaped hybrid composite electrodes by core-shell electrospinning. ChemNanoMat **5**, 792–801 (2019)
62. Poudeh, L.H., Cakiroglu, D., Cebeci, F.C., Yildiz, M., Menceloglu, Y.Z., Okan, B.S.: Design of Pt-supported 1D and 3D multilayer graphene-based structural composite electrodes with controlled morphology by core-shell electrospinning/electrospraying. ACS Omega **3**, 6400–6410 (2018)
63. Huang, Y., Lai, F., Zhang, L., Lu, H., Miao, Y.-E., Liu, T.: Elastic carbon aerogels reconstructed from electrospun nanofibers and graphene as three-dimensional network matrix for efficient energy storage/conversion. Sci. Rep. **6**, 31541 (2016)
64. He, S., Chen, L., Xie, C., Hu, H., Chen, S., Hanif, M., Hou, H.: Supercapacitor based on 3D network of activated carbon nanowhiskers wrapped-on graphitized electrospun nanofiber. J. Power Sour. **243**, 880–886 (2013)
65. Kim, T.-W., Park, S.-J.: Synthesis of reduced graphene oxide/thron-like titanium dioxide nanofiber aerogels with enhanced electrochemical performances for supercapacitor. J. Colloid Interface Sci. **486**, 287–295 (2017)
66. Tai, Z., Yan, X., Lang, J., Xue, Q.: Enhancement of capacitance performance of flexible carbon nanofiber paper by adding graphene nanosheets. J. Power Sour. **199**, 373–378 (2012)
67. Dong, Q., Wang, G., Hu, H., Yang, J., Qian, B., Ling, Z., Qiu, J.: Ultrasound-assisted preparation of electrospun carbon nanofiber/graphene composite electrode for supercapacitors. J. Power Sour. **243**, 350–353 (2013)
68. Chee, W.K., Lim, H.N., Zainal, Z., Harrison, I., Andou, Y., Huang, N.M., Altarawneh, M., Jiang, Z.T.: Electrospun graphene nanoplatelets-reinforced carbon nanofibers as potential supercapacitor electrode. Mater. Lett. **199**, 200–203 (2017)
69. Rose, A., Raghavan, N., Thangavel, S., Maheswari, B.U., Nair, D.P., Venugopal, G.: Investigation of cyclic voltammetry of graphene oxide/polyaniline/polyvinylidene fluoride nanofibers prepared via electrospinning. Mater. Sci. Semicon. Process. **31**, 281–286 (2015)
70. Rose, A., Prasad, K.G., Sakthivel, T., Gunasekaran, V., Maiyalagan, T., Vijayakumar, T.: Electrochemical analysis of graphene oxide/polyaniline/polyvinyl alcohol composite nanofibers for supercapacitor applications. Appl. Surf. Sci. **449**, 551–557 (2018)
71. Chen, L., Chen, L., Ai, Q., Li, D., Si, P., Feng, J., Zhang, L., Li, Y., Lou, J., Ci, L.: Flexible all-solid-state supercapacitors based on freestanding, binder-free carbon nanofibers@polypyrrole@graphene film. Chem. Eng. J. **334**, 184–190 (2018)
72. Chee, W.K., Lim, H.N., Andou, Y., Zainal, Z., Hamra, A.A.B., Harrison, I., Altarawneh, M., Jiang, Z.T., Huang, N.M.: Functionalized graphene oxide-reinforced electrospun carbon nanofibers as ultrathin supercapacitor electrode. J. Energ. Chem. **26**, 790–798 (2017)

73. Zhou, Z., Wu, X.-F.: Graphene-beaded carbon nanofibers for use in supercapacitor electrodes: synthesis and electrochemical characterization. J Power Sour. **222**, 410–416 (2013)
74. Qiu, X., Xiao, Z., Wang, L., Fan, L.-Z.: High rate integrated quasi-solid state supercapacitors based on nitrogen-enriched active carbon fiber/reduced graphene oxide nanocomposite. Carbon **130**, 196–205 (2018)
75. Thangappan, R., Kalaiselvam, S., Elayaperumal, A., Jayavel, R.: Synthesis of graphene oxide/vanadium pentoxide composite nanofibers by electrospinning for supercapacitor applications. Solid State Ion. **268**, 321–325 (2014)
76. Lee, D.G., Kim, B.-H.: MnO_2 decorated on electrospun carbon nanofiber/grapheme composites as supercapacitor electrode materials. Synth. Met. **219**, 115–123 (2016)